

Representation Bayesian Risk Decompositions and Multi-Source Domain Adaptation

Xi Wu², Yang Guo¹, Jiefeng Chen¹, Yingyu Liang¹, Somesh Jha^{1,3}, and Prasad Chalasani³

¹University of Wisconsin-Madison

²Google

³XaiPient

Abstract

We consider representation learning (with hypothesis class $\mathcal{H} = \mathcal{F} \circ \mathcal{G}$) where training and test distributions can be different. Recent studies provide hints and failure examples for domain invariant representation learning, a common approach to this problem, but are inadequate for fully understanding the phenomena. In this paper, we provide new decompositions of risk which provide finer-grained explanations and clarify potential generalization issues. For Single-Source Domain Adaptation, we give an *exact* risk decomposition, an *equality*, where target risk is the sum of three factors: (1) *source risk*, (2) *representation conditional label divergence*, and (3) *representation covariate shift*. We derive a similar decomposition for the Multi-Source case. These decompositions reveal factors (2) and (3) as the precise reasons for failing to generalize. For example, we demonstrate that domain adversarial neural networks (DANN) attempt to regularize for (3) but miss (2), while a recent technique Invariant Risk Minimization (IRM) attempts to account for (2) but may suffer from not considering (3). We also verify these observations experimentally.

1 Introduction

Representation learning has emerged as a promising approach for machine learning in domain adaptation [1, 2] (for a more recent analysis of this line, see [3] and references therein). A common setup is to consider a hypothesis class \mathcal{H} that can be decomposed into $\mathcal{F} \circ \mathcal{G}$, where \mathcal{F} is a class of predictors which map representations to predictions¹, and \mathcal{G} is a class of representations which map the input to representations. Compared to using a monolithic hypothesis class, using representations provides a new level of abstraction to study properties of information useful for adapting to different domains [4], including computer vision [5, 6] and natural language processing [7, 8].

A theme of representational domain adaptation is to derive a *risk decomposition* that involves representations, and use it to guide the search of desired representations. For example, a popular decomposition in single-source case is Domain Invariant Representations (DANN [2]):

$$R^t(f \circ \phi) \leq R^s(f \circ \phi) + d(\Phi^s, \Phi^t) + \lambda_{\mathcal{H}}^*$$

which says that target risk is bounded by three factors: (1) source risk, (2) distance between set of feature representations Φ^s and Φ^t , and (3) a term $\lambda_{\mathcal{H}}^*$ that solely depends on the overall hypothesis class \mathcal{H} (and thus is regarded as unlearnable).

However, recent work [3, 9, 10] has pointed out that the term $\lambda_{\mathcal{H}}^*$ hides information about different choices of representations, and thus may not be informative about the failure cases of domain invariant representations. This work proposed the failure examples and possible explanations (e.g., [3] proposed an explanation based on input support misalignment). None of the existing work, on the other hand, proposed revised risk decompositions where these failures *can surface as factors in the decompositions*.

¹In this work, we assume that the predictors output a probability vector over the labels, which corresponds to the output of softmax layer in typical classifiers, including deep neural networks.

In this paper we take a step to bridge this gap. We derive new risk decompositions that are more fine-grained and can clarify failure examples by mapping them to exact factors in the decompositions. Our key idea is that since representation class \mathcal{G} provides an intermediate abstraction, it is fundamental to understand the following question:

What is the information that $\phi \in \mathcal{G}$ outputs for domain adaptation?

1.1 Overview of our theory and results

As a first approach to answer the question, we propose to examine Bayesian optimal predictors over $\phi \in \mathcal{G}$ (in different domains, respectively). This allows us to examine distributions produced by ϕ in different domains, and give risk decompositions that are “purely representational.”

Single-Source Domain Adaptation (SSDA). We first use this view to examine Single-Source Domain Adaptation.

1. We first derive an *exact decomposition* (*an equality*) which says that the target risk is the sum of three factors: (1) source risk, (2) representation conditional label divergence, and (3) representation covariate shift.
2. This equality allows us to explain failure examples found in [3, 9] as exactly a large conditional divergence (factor (2)), and is information-theoretically impossible to solve without target labeled data. This indicates that domain invariant representation approach (e.g. DANN) attempt to regularize (3) but misses (2), and there is a *fundamental limitation* of Single-Source Domain Adaptation with only *unlabeled* data from the target domain.
3. We use our theory to analyze the *success* of DANN for MNIST→MNIST-M. That is, the source domain is the MNIST data set and the target domain is the MNIST-M dataset, created by replacing the background of MNIST with colored images and thus, similar to the failure example presented in, the input support of two domains is disjoint. Nevertheless, DANN can succeed for this domain adaptation task. Through the lens of the exact decomposition, the success of DANN on MNIST→MNIST-M also has an immediate explanation: *The perfect representation alignment (i.e. factor (3) = 0) in this case implies conditional label alignment (i.e. factor (2) = 0)*.
4. Finally, we give an upper bound of covariate shift as “source fairness \times representation divergence”. This uncovers more possible failure cases of domain invariant representation, where some of which have been pointed out in [10]. This also highlights the importance of source fairness if representation distributions have intrinsic misalignment.

Multi-Source Domain Adaptation (MSDA). We then extend our results to Multi-Source Domain Adaptation.

1. Multiple training distributions allow us to observe conditional label divergence. We derive a risk decomposition that target risk is bounded by conditional label divergence and covariate shift in the training domains, plus a term called predictor adaptation distance quantifying whether these alignments in the source domains can generalize to the test domain.
2. Our decomposition motivates a property which we term the *Environment Conditional Invariance (ECI)*. We show that ECI is essentially equivalent to the Invariant Risk Minimization (IRM) [10], if the loss function satisfies some natural properties. However, we prefer focusing on ECI since it is a property of representations themselves and does not depend on an optimization formalization.
3. Our decomposition reveals that IRM considers exactly perfect conditional label alignment (factor (2)), but misses representation covariate shift (factor (3)), and thus its performance may be hurt due to that, which is verified in our experiments (Figure 4). We further note that generalization to the target can fail when the predictor adaptation distance is large. We demonstrate this via an “distribution memorization problem” (Prop 1 and Section B.2).

Implications of our theory. We provide a discussion on various implications of our theory. We argue that our theory provides a unified understanding of domain adaptation based on representations, and highlights that conditional label divergence and covariate shift (which further factors into fairness and representation divergence) at the representation level need to be considered in a synergetic way. We believe that this view provides an avenue for future research.

2 Related Work

Representation learning has become a popular approach for various applications, and learning invariant representations across multiple domains has been a popular method for domain adaptation in recent years. A classic approach for analyzing domain adaption is based on \mathcal{H} -divergence [11, 12, 13]. That theoretical framework is the basis for a line of methods that uses adversarial training with neural networks to learn representations that are indistinguishable between source and target domain, in particular domain adversarial neural network (DANN) [14, 15] and related techniques [16, 17, 18]. Some other approach used different divergence notions, such as MMD [19, 20], Wasserstein distance [21, 22], and Rényi divergence [23]. Another line of research for domain adaptation is based on causal approaches that typically assume shared generative distributions, e.g., [24, 25, 26]. This work instead focuses on discriminative representation learning and does not make generative assumptions.

On the other hand, the \mathcal{H} -divergence bound is for general learning rather than representation learning, and thus falls short in explaining some failure cases. [27, 3] both pointed out the insufficiency of learning domain-invariant representation. [3] proposed a generalization upper bound that considers the information loss of non-invertible transformations. [27] derived an information-theoretic lower bound of the joint error on the source and target domains and demonstrated that invariant representations do not necessarily lead to generalization in the target domain when the label distributions differ significantly. Our work provides an exact risk decomposition for domain adaptation which further clarifies the factors leading to the failure of generalization.

Invariant Risk Minimization (IRM) [28] proposed to learn representations that result in the same optimal prediction across domains. We noted that this corresponds to enforcing one factor in our risk decomposition, which also reveals conditions for success and suggests potential improvements to IRM.

3 Preliminaries

Domain adaptation. Single-source domain adaptation has a source domain s and a target domain t . Each domain is a distribution over a set of feature vectors and labels. In the multi-source case, we have a set of source domains \mathcal{E}_{tr} , and one target domain e_0 for testing. Given a representation ϕ , we use Φ^e to denote the random vector $\phi(X^e)$ where X^e is the random variable distributed according to the input feature distribution in the environment e .

Cross entropy function and cross entropy loss. For simplicity of developing and presenting results, throughout this paper we will work with cross entropy loss. However, our results can be extended in a straightforward way to other loss functions. Given two distribution p, q , cross entropy function $H_p(q)$ is defined as $H_p(q) = \sum_i q_i \log \frac{1}{p_i}$. We also use cross entropy loss function where for a label $y \in [K]$, and a probability vector $p \in \Delta_K$, $\ell(p, y) = H_p(\mathbf{1}_y) = \log \frac{1}{p_y}$, where $\mathbf{1}_y$ is a K -dimensional vector with y -th component 1, and 0 otherwise. Given an environment e with distribution X^e, Y^e , and a hypothesis $h \in \mathcal{F} \circ \mathcal{G}$, we define its population risk over e , $R^e(h)$ as $\mathbb{E}[\ell(h(X^e), Y^e)]$.

Representation Bayesian optimal predictors. Given $\phi \in \mathcal{G}$, we denote by f_ϕ^e the Bayesian optimal predictor on top of the representation $\phi(X^e)$ in environment e . That is, $f_\phi^e(\gamma)$ outputs a probability vector such that for $y \in [K]$, $[f_\phi^e(\gamma)]_y = \Pr[Y^e = y | \phi(X^e) = \gamma]$. In other words, $f_\phi^e(\gamma) = (Y^e | \phi(X^e) = \gamma)$, the label distribution conditioned on $\phi(X^e) = \gamma$. To simplify notation, we simply use $Y^e | \gamma^e$.

Aligning representation support. For convenience, throughout the paper (unless stated otherwise), we assume that the support of X^e for all the environments e is \mathbb{R}^d , so the support of $\phi(X^e)$ in all e is the same for any ϕ .² Formally, we make the following minimal assumption on aligning representation support.

Assumption 1 (Representation Support Alignment). *A representation ϕ is said to align the support if $\text{supp}(\phi(X^s)) = \text{supp}(\phi(X^t))$. In the rest of the paper we let Ω denote the aligned representation support.*

²This is essentially without loss of generality, since we can consider a smooth version of e which is a mixture of e with weight $1 - \epsilon$ and the standard Gaussian distribution with weight ϵ for an arbitrarily small $\epsilon > 0$.

4 Single-Source Domain Adaptation

In this section, we derive representation risk decompositions in the setting with a single training distribution and use them to clarify failure examples found for invariant representation learning. This section is organized as follows:

1. We start by introducing two categories of quantities, *representation conditional label divergence* and *representation covariate shift*. These quantities are defined based on the Bayesian optimal predictors over ϕ , and thus reflect the distributions produced by ϕ on the source and target domains.
2. We use these quantities to give an exact risk decomposition, an *equality*, for target risk where we use the optimal source predictor given ϕ . We further show that the representation covariate shift can be naturally decomposed (and upper bounded) by the *product* of two quantities: *representation source fairness* and *representation divergence*.
3. We use the decomposition derived in (1) and (2) to explain and clarify failure examples found in [3, 9], and some variants not considered in those work. Our decomposition gives finer-grained explanations which map failures exactly to factors in the decompositions. Interestingly, our decompositions also allow us, for the first time, to explain some natural *success* cases of invariant representation.
4. Finally, we consider Conditional Domain Invariant Representation [29]. We point out the problem of inherent representation misalignment and the importance of source fairness in view of that.

4.1 Quantities for Decomposition

Representation conditional label divergence. Given a representation ϕ , and a value γ that ϕ may take, the conditional label distributions $Y^t|\gamma^t$ and $Y^s|\gamma^s$ may differ. To measure the expected divergence of these conditional label distributions, we introduce two quantities, representation domain KL divergence, and representation domain Bayesian divergence.

Definition 1 (Representation Domain KL-divergence). *We define (representation) domain KL-divergence as $\text{KL}_{\phi}^{s,t} := \int_{\Omega} d_{\text{KL}}(f_{\phi}^t(\gamma) \parallel f_{\phi}^s(\gamma)) \mu^t(d\gamma)$. where d_{KL} is the KL divergence. Symmetrically, we define $\text{KL}_{\phi}^{t,s}$ by swapping s, t .*

Definition 2 (Representation Domain Bayesian divergence). *We define (representation) domain Bayesian divergence as $\delta_{\phi}^{s,t} := \int_{\Omega} (H(Y^t|\gamma^t) - H(Y^s|\gamma^s)) \mu^t(d\gamma)$. Symmetrically, we define $\delta_{\phi}^{t,s}$ by swapping s, t .*

Representation covariate shift. Representation conditional label divergence considers the case where we fix the representation distribution but vary conditional label distributions. By symmetry, we can also consider fixing the conditional label distributions, but vary the underlying representation distribution. This gives the following definition:

Definition 3 (Representation covariate shift). *We define s - t representation covariate shift, denoted as $\mu_{\phi}^{s,t}$, as $\mu_{\phi}^{s,t} = \int_{\Omega} H(Y^s|\gamma^s) \mu^t(d\gamma) - \int_{\Omega} H(Y^s|\gamma^s) \mu^s(d\gamma)$. In other words, we consider representation distribution changing from Φ^s to Φ^t , while fixing conditional label distribution as $Y^s|\gamma^s$.*

4.2 Single-Source Representation Risk Decomposition

Our single-source decomposition uses a hybrid argument based on a natural hybrid called s - t mixture. Intuitively, this hybrid distribution retains the same representation distribution as that of the target, but switch the label distribution conditioned on a representation to that of the source. Formally, it is defined as follows:

Definition 4 (s - t Mixture). *An s - t mixture, denoted as (Φ^m, Y^m) , is a distribution defined on the $\Omega \times [K]$ (representation support times label space) as follows:*

- Φ^m and $\Phi^t = \phi(X^t)$ are same distributed. That is the feature distribution follows the target domain.
- On the other hand, $Y^m|\gamma^m = Y^s|\gamma^s$. That is the conditional label distribution follows the source domain.

We are ready to present an exact decomposition:

Theorem 1 (Exact Decomposition). *We have that*

$$R^t(f_\phi^s \circ \phi) = \underbrace{R^s(f_\phi^s \circ \phi)}_{\text{source error}} + \underbrace{\text{KL}_\phi^{s,t} + \delta_\phi^{s,t}}_{\text{conditional label div}} + \underbrace{\mu_\phi^{s,t}}_{\text{covariate shift}}$$

That is, target risk equals the sum of (1) source risk, (2) representation conditional label divergence, and (3) representation covariate shift.

Proof. We decompose $R^t(f_\phi^s \circ \phi) - R^s(f_\phi^s \circ \phi)$ as

$$\begin{aligned} R^t(f_\phi^s \circ \phi) - R^s(f_\phi^s \circ \phi) &= (R^t(f_\phi^s \circ \phi) - R^t(f_\phi^t \circ \phi)) \\ &\quad + (R^t(f_\phi^t \circ \phi) - R^m(f_\phi^s \circ \phi)) \\ &\quad + (R^m(f_\phi^s \circ \phi) - R^s(f_\phi^s \circ \phi)). \end{aligned}$$

One can then verify that $R^t(f_\phi^s \circ \phi) - R^t(f_\phi^t \circ \phi) = \text{KL}_\phi^{s,t}$, $R^t(f_\phi^t \circ \phi) - R^m(f_\phi^s \circ \phi) = \delta_\phi^{s,t}$, $R^m(f_\phi^s \circ \phi) - R^s(f_\phi^s \circ \phi) = \mu_\phi^{s,t}$. \square

Upper bounding representation covariate shift by fairness and representation divergence. Next we study the term $\mu_\phi^{s,t}$. We note that $H(Y^s | \gamma^s)$ is a function of γ . An important point is that this function *only* depends on the *source domain*. We consider the following definition:

Definition 5. The (Representation) Source Fairness, ρ_ϕ^s , is defined as $\rho_\phi^s := \sup_{\gamma \in \Omega} \{H(Y^s | \gamma^s)\}$.

Source fairness quantifies the intrinsic difficulties of ϕ in discriminating certain inputs (that is, even the Bayesian optimal predictor over ϕ cannot discriminate the inputs mapped to γ well). Importantly, this quantity *only* depends on the *source domain*, and so it is learnable using labeled source data. Finally, observe that $\rho_\phi^s \leq \log K$, where the maximal is achieved when $Y^s | \gamma$ is a uniform distribution over $[K]$. This leads to the following bound on covariate shift:³

Corollary 1.

$$\mu_\phi^{s,t} \leq \underbrace{\rho_\phi^s}_{\text{repr. source fairness}} \times \underbrace{d_{\text{TV}}(\Phi^s, \Phi^t)}_{\text{repr. divergence}}$$

Proof. Note that $\kappa(\gamma) := H(Y^s | \gamma^s) / \rho_\phi^s$ is a function bounded by 1, and $\mu_\phi^{s,t}$ is indeed $\rho_\phi^s \cdot \left(\int_{\Omega} \kappa(\gamma) \mu^t(d\gamma) - \int_{\Omega} \kappa(\gamma) \mu^s(d\gamma) \right)$, which is bounded by $\rho_\phi^s \cdot d_{\text{TV}}(\Phi^s, \Phi^t)$ where $d_{\text{TV}}(\Phi^s, \Phi^t)$ is the total variation distance between Φ^s and Φ^t . \square

Factors for failing to generalize. Our analysis suggests that the gap between source and target-error can be upper bounded as “*conditional-label-divergence + source-fairness × representation-divergence*.” Therefore there are two failure factors to generalize:

Large representation conditional label divergence. Even if one achieves perfect covariate shift, one may still have large target error due to conditional label divergence.

Large representation covariate shift. Even if ϕ aligns perfectly the conditional label distributions, one may still have a error in target environment due to covariate shift. Specifically, this can happen if ϕ provides bounds for neither ρ_ϕ^s nor $d_{\text{TV}}(\Phi^s, \Phi^t)$. In other words, covariate shift could be minimized if either (1) we can find a ϕ to align representations, or (2) if there is no such ϕ for (1), but ρ_ϕ^s can be bounded over representation ϕ .

Comparison with existing risk decompositions. We now compare Theorem 1 with existing decompositions. We consider (T1) Theorem 1 [13], (T2) Theorem 4.1 [27], and (T3) Theorem 2 [3].

The Bayes classifier and our other notions (Def 1 to 3) are defined w.r.t. the representation. For both (T1) and (T2), the notions are w.r.t. the input space (e.g., “Notations” and “Comparison with Theorem 2.1” in [27]). Working

³Section A.1 in the appendix gives a tighter bound based on group fairness instead of point-wise fairness.

at representation level allows us to examine different representation conditional distributions in a hypothesis class of representations. (T1) and (T2) do not formulate representation class.

Our bound is tighter even if one argues to apply (T1) and (T2) at the representation level. This is because an equality implies that our terms must be reflected in any valid upper bound, but still, an equality can provide more thorough insights. For (T1), please refer to Appendix E for a detailed comparison. The insufficiency of (T1) has also been discussed in several existing works (including [27, 3]).

For (T2), we note two points: (i) Our decomposition is an “orthogonal decomposition” but (T2) is not. Specifically, our conditional label divergence terms (Def 1 and 2) are not be affected by representation covariate shift since both integrals are only evaluated over the target representation distribution. By contrast, while the third term in (T2) is related to conditional label divergence, it depends on both source and target representation distributions, and so mixes conditional label divergence and covariate shift. (ii) While the second term in (T2) can be interpreted as covariate shift over representations, our term provides new implications. Corollary 1 shows that a big TV distance between the target/source representation distributions may not affect the target risk if the source fairness is zero. This is not known in previous work, including (T2).

(T3) is the closest decomposition to ours, and their terms offer different upper bounds for our representation covariate shift and representation conditional label divergence. Specifically, the upper bound for representation covariate shift is different from our Corollary 1. This again demonstrates the benefits of our equality decomposition which gives new insights for failure scenarios as described above.

4.3 An Analysis of Domain Invariant Representations

Invariant representation is a popular approach for Single-Source Domain Adaptation. As in [3, 9], we consider the following objective (for example, see DANN [2]):

$$\underset{\phi \in \mathcal{G}, f \in \mathcal{F}}{\text{minimize}} \quad R^s(f \circ \phi) + \lambda \cdot d(\Phi^s, \Phi^t) \quad (1)$$

where $\lambda > 0$ is a regularization parameter and d is a distance function between two distributions. The objective is to essentially minimize the source risk with a regularization term based on the distance between the distribution of the source and target. In this section we perform an analysis of failure cases found in recent work and also consider some new variants. Our analysis is structured as follows:

1. We first revisit a failure example found in both [3, 9]. Using our exact decomposition (Theorem 1), we map the failure reason precisely to representation conditional label divergence. We note that [9] provided a similar reason to ours, though their risk decomposition (see Their Theorem 4.1) is not exact.
2. We then use our theory to analyze the *success* of DANN for MNIST→MNIST-M. In this case, the source domain is the MNIST data set and the target domain is the MNIST-M dataset, which is obtained by replacing background of MNIST images by colored images. Similar to the above failure example, the input support of two domains is *disjoint*, but nevertheless DANN can still succeed. We show that the essential reason behind this success is that in this case representation alignment implies conditional label alignment.

Example 1 (Failure Example from [3, 9]). Consider input space $\mathcal{X} = [-1, 1] \times [-1, 1]$, $\mathcal{G} = \{\phi_1, \phi_2\}$ where $\phi_1(x) = x_1$ and $\phi_2(x) = x_2$ (that is these two representations are projections on the two axes), and $\mathcal{F} = \{\mathbf{1}_\lambda(\cdot)\}$ (that is we consider thresholding functions that $\mathbf{1}_\lambda(\alpha) = 1$ if $\alpha > \lambda$, and 0 otherwise. The source domain s puts a uniform distribution in the second and fourth quadrants, and has label 1 in the second quadrant, and label 0 in the fourth quadrant. On the other hand, target distribution t puts a uniform distribution in the first and third quadrant, and has label 1 in the first quadrant and label 0 in the third quadrant (See Figure 1).

Clearly, the underlying truth is $\phi_2(x) = x_2$, which perfectly classifies both source and target data. However, with Single-Source Domain Adaptation where we only have unlabeled data from the target domain, using (1) we cannot distinguish between ϕ_1 and ϕ_2 : Both of them have zero risk on the source domain, and both give perfect alignment between Φ^s and Φ^t . (i.e., both perfectly minimize (1)).

Our explanation using conditional label divergence. Our exact representation risk decomposition (Theorem 1) provides an immediate explanation for Example 1: ϕ_1 has a large representation conditional label divergence. Since

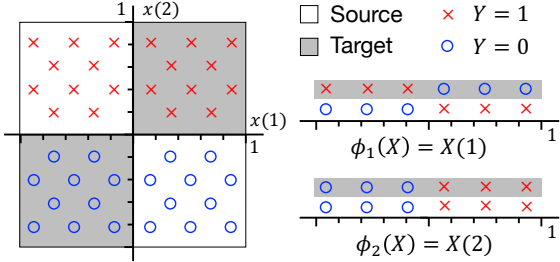


Figure 1: Variable selection example in [3] that DANN will fail to learn. Specially, objective 1 will have two different optimal solutions with very different target risks. The figure comes from [3].

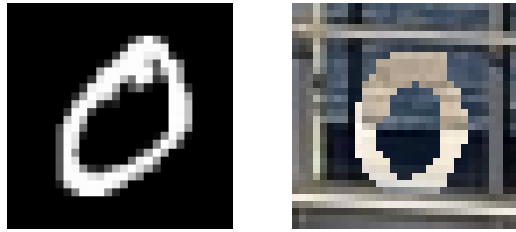


Figure 2: MNIST-M images (right) are obtained from MNIST images (left) by replacing the black background with random images. As a result, MNIST and MNIST-M have disjoint input support. The figure comes from [3].

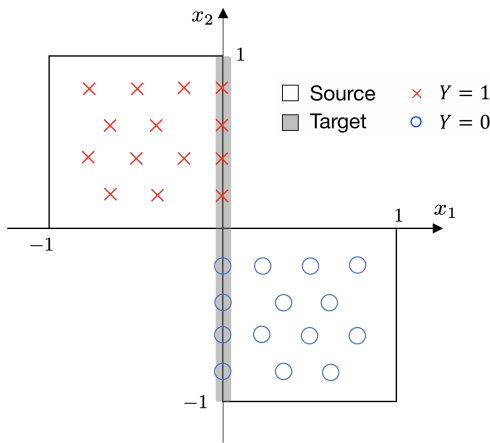


Figure 3: An artificial example which captures the phenomenon where representation alignment may trivially imply conditional label alignment, the reason why DANN works for MNIST \rightarrow MNIST-M. The source domain in this example is the same as that in Example 1, but the target domain has $x_1 = 0$. Therefore, x_2 is the only signal that can be used as representation to align two domains (this is similar to the digit signal in MNIST \rightarrow MNIST-M). Further, since x_2 is the right signal for prediction, aligning representation implies conditional label alignment.

we only have one source domain, and do not have labeled data from the target domain, it is information theoretically impossible to align conditional label distributions, and thus distinguish between ϕ_1 and ϕ_2 . To this end, we note that [9] mentioned a similar explanation based on their Theorem 4.1. As we have discussed in the previous section, our exact decomposition at representation level provides a more precise explanation (representation covariate shift is zero while conditional label divergence is large).

DANN on MNIST \rightarrow MNIST-M: Representation alignment implies conditional label alignment. One may argue that the failure of the above example is because that, at the input level, the support of source and target domains is completely disjoint. To this end, we note that there is a successful case of invariant representation learning that is nevertheless of this nature. Specifically, DANN succeeds in MNIST \rightarrow MNIST-M, where MNIST-M is a dataset created from MNIST by replacing the background images with colored images, which causes the support of two domains at the input level to be disjoint.

Through the lens of the exact decomposition, the success of DANN on MNIST \rightarrow MNIST-M also has an immediate explanation: *The representation alignment in this case trivially implies conditional label alignment.* Merely replacing background images will make digit representation the only discriminative signal that exists in both source and target.

Therefore by finding the only representation that could align the two domains, the conditional label alignment is trivially implied (because digit representation is the causal representation for prediction). This phenomenon is captured by the following example:

Example 2 (Representation alignment implies conditional label alignment). *We consider the same setting as in Example 1. However, for target domain, we have uniform distribution over $\{0\} \times [-1, 1]$, and for $\{(0, x_2) \mid 0 < x_2 < 1\}$ we give label 1, and for $\{(0, x_2) \mid -1 < x_2 < 0\}$ we give label 0. In other words, the probability mass, instead of spreading over the second and the fourth quadrants, it concentrates on the x_2 axis.*

In this case, only $\phi_2(x) = x_2$ aligns the representation distributions, since $\phi_1(x) = x_1$ will be constantly 0 for the unlabeled data from the target domain, which has measure 0 in the source data when projecting to x_1 . DANN will thus learn x_2 which perfectly classifies the target data.

4.4 Variants, Representation Alignment, and Fairness

Intrinsic representation misalignment. Some recent proposals (for example, [29]) considered modifying (1) to align the conditional representation distributions, $\Phi^s|Y^s$ and $\Phi^t|Y^t$, instead of Φ^s and Φ^t . However, in view of our decomposition, these works may all suffer from one problem: *Objectively there may be no representation alignment even for the underlying truth representation.* For example, for the above two examples, one can modify the digit distributions (which is the causal representation) so that they are objectively misaligned between source and target (one can do so even for conditional representations). In these cases, learning using (1) or its conditional variants will have inherently large risk. We note that the recent work of Invariant Risk Minimization [10] has provided a similar observation (see Appendix C of their paper), but however did not map it to a risk decomposition factor.

Covariate shift and source fairness. The possibly intrinsic representation misalignment is exactly caused by representation covariate shift in Theorem 1. If one has no control over that, then to control covariate shift one has to find a ϕ with small source fairness. That is, ϕ should not discriminate different γ with a too large a gap. In fact, Corollary 1 suggests that under the assumptions that: (1) target risk is large, (2) source risk is small, (3) conditional label divergence is small, (4) representation divergence is objectively large, then source fairness must be large.

5 Multi-Source Domain Adaptation

The analysis in the single-source setting suggests that we should minimize both the conditional label divergence and the representation covariate shift. The former, however, generally requires labels from the target domain which are not available. A natural idea is to consider multiple sources among which we can minimize the conditional label divergence. So we now turn to the setting with multiple sources \mathcal{E}_{tr} and one target domain e_0 , and we focus on the case where no data from the target domain is available for training. We generalize the risk decomposition bound in the single-source setting, discuss its implications for invariant representation learning and the connection to recently proposed approach IRM (invariant risk minimization), and present and clarify the conditions for success. Specifically:

1. We start by introducing a new quantity, *predictor adaptation gap* between the target and the sources, which measures how “far” the target is from the sources. If it is small, then learning over sources can generalize to the target. We then use this quantity and the bound from the single-source setting to derive the multi-source risk bound.
2. We then review a natural regularization called *environment conditional invariance* (ECI) implied by the bound to learn invariant representation using multiple sources. We show that this is essentially the recently proposed method, Invariant Risk Minimization (IRM).
3. We present examples under which IRM can fail to generalize, and use the decomposition derived above to explain and clarify the root causes. We point out that the performance of IRM can be hurt by representation covariate shift, which is verified in experiments. Furthermore, we describe a *distribution memorization* phenomena where a hypothesis class that is too large can prevent generalization to the target despite all benign assumptions about the data and optimization. We verify this implication in experiments and also verify that this issue can be alleviated via a simple pre-training heuristic.

5.1 Multi-Source Representation Risk Decomposition

Ideally, one would like to bound the target risk by terms that can be optimized on the source environments, which can be used as regularization for learning even when no data from the target domain is available. However, generalization to an arbitrary target is not possible, so there must be some condition on the target, which will be reflected by a term quantifying the condition in the risk bound. We begin by introducing such a quantity: **Predictor Adaptation Gap**. We first introduce the notion for two distributions, and then define it between the target and the sources.

Definition 6. Define the predictor adaptation gap between two distributions e_1 and e_2 with respect to a representation function ϕ and \mathcal{E}_{tr} as $d_\phi(e_1, e_2; \mathcal{E}_{\text{tr}}) := \sup_{e \in \mathcal{E}_{\text{tr}}} R^{e_1}(f_\phi^e \circ \phi) - R^{e_2}(f_\phi^e \circ \phi)$.

To get some intuition, suppose this gap is small. If $f_\phi^e \circ \phi$ learned on e can be used in e_2 (i.e., $R^{e_2}(f_\phi^e \circ \phi)$ is small), then it can also be used in e_1 (i.e., $R^{e_1}(f_\phi^e \circ \phi)$ is also small).

Definition 7. Define the predictor adaptation gap between e_0 and \mathcal{E}_{tr} with respect to ϕ as:

$$d_\phi(e_0, \mathcal{E}_{\text{tr}}) := \inf_{e' \in \mathcal{E}_{\text{tr}}} d_\phi(e_0, e'; \mathcal{E}_{\text{tr}}).$$

For convenience of discussion, we also define the predictor adaptation gap between e_0 and \mathcal{E}_{tr} over the whole class \mathcal{G} as $d_{\mathcal{G}}(e_0, \mathcal{E}_{\text{tr}}) := \sup_{\phi \in \mathcal{G}} d_\phi(e_0, \mathcal{E}_{\text{tr}})$.

We are ready to present our risk decomposition:

Theorem 2. For any ϕ , we have

$$\sup_{e \in \mathcal{E}_{\text{tr}}} R^{e_0}(f_\phi^e \circ \phi) \leq \underbrace{\sup_{e \in \mathcal{E}_{\text{tr}}} R^e(f_\phi^e \circ \phi)}_{\text{source error}} + \underbrace{\sup_{e, e' \in \mathcal{E}_{\text{tr}}} [\delta_\phi^{e, e'} + \text{KL}_\phi^{e, e'} + \mu_\phi^{e, e'}]}_{\text{cond. label div. + covariate shift}} + \underbrace{d_\phi(e_0, \mathcal{E}_{\text{tr}})}_{\text{predictor adaptation gap}}.$$

The risk bound has three parts: (1) Source risk. The supremum over $e \in \mathcal{E}_{\text{tr}}$ is necessary for getting a small target risk, if the set of possible targets e_0 includes \mathcal{E}_{tr} . The other two terms quantify the generalization to targets outside \mathcal{E}_{tr} . (2) Conditional label divergence and covariate shift of the representations among the sources. Assuming that there exists a ground-truth function $f^* \circ \phi^*$ that is simultaneously good for all distributions, this part can be used for regularization (see the next subsection). (3) The “generalization gap” due to the distribution shift from the sources and the target. This term is the key factor determining generalization to new domains/distributions beyond the sources \mathcal{E}_{tr} considered in the training. If the target e_0 does not align with \mathcal{E}_{tr} , then in the worst case we cannot expect the learned hypothesis to generalize to e_0 . On the other hand, when e_0 aligns with some source in \mathcal{E}_{tr} , then generalization is possible.

The bound also shows a trade-off between the generalization gap and the other two terms. A larger \mathcal{E}_{tr} potentially leads to a smaller gap but larger source risks, larger label divergence and covariate shift among the sources, and harder optimization. Similarly, the bound implicitly shows a larger hypothesis class \mathcal{G} potentially leads to smaller source risks but a larger gap. To see this, suppose the optimization method successfully finds a $\hat{\phi}$ with small source risks, and small conditional label divergence and covariate shift among the sources. Then, the generalization gap is $d_{\hat{\phi}}(e_0, \mathcal{E}_{\text{tr}})$, which can be as large as $\sup_{\phi \in \mathcal{G}} d_\phi(e_0, \mathcal{E}_{\text{tr}})$ in the worst case. So a larger hypothesis class \mathcal{G} potentially leads to a larger gap.

5.2 Conditional Label Divergence and Invariant Risk Minimization

Our theorem leads to the following question: how does one regularize to minimize the terms? Here we consider the representation conditional label divergence. The extreme is to make the conditional label distribution on the representation to be the same across e and e' , which will make the label divergence (both terms $\delta_\phi^{e, e'}$ and $\text{KL}_\phi^{e, e'}$) zero.

Definition 8 (Environment Conditional Invariance). A representation ϕ satisfies environment conditional invariance (ECI) w.r.t. distribution family \mathcal{E} if $\forall e, e' \in \mathcal{E}, \forall r \in \text{supp}(\phi(X^e)) \cap \text{supp}(\phi(X^{e'}))$, $\forall y \in [K]$, $\Pr[Y^e = y | \phi(X^e) = r] = \Pr[Y^{e'} = y | \phi(X^{e'}) = r]$.

ECI means that the Bayesian optimal prediction function on the representation (i.e., $\Pr[Y^e|\phi(X^e)]$) is invariant across all the distributions. This is a natural assumption on the representation ϕ and thus is a particularly useful inductive bias for invariant learning. Previous work has provided extensive motivation. It is closely related to the notion of invariant prediction in [30], and has been mentioned in recent work (e.g., [31]).

Furthermore, recent work [10] has proposed and studied a closely related notion that representation ϕ leads to the existence of a predictor *simultaneously optimal* for all the domains (called ϕ eliciting an invariant predictor). Based on this, an approach called Invariant Risk Minimization (IRM) is proposed and obtained interesting experimental results:

$$\begin{aligned} \min_{h \in \mathcal{F}, \phi \in \mathcal{G}} \quad & \sum_{e \in \mathcal{E}_{\text{tr}}} R^e(h \circ \phi), \\ \text{subject to} \quad & h \in \arg \min_{h \in \mathcal{F}} R^e(h \circ \phi) \quad \text{for } \forall e \in \mathcal{E}_{\text{tr}}. \end{aligned}$$

This is empirical risk minimization subject to *simultaneous optimality* of the predictor for all sources. As pointed in [10], when the loss has the property that the minimizer is the Bayesian optimal predictor and \mathcal{F} is large enough to include that, ECI and simultaneous optimality are equivalent.⁴ In this case, let \mathcal{G}_I denote the subset of hypotheses in \mathcal{G} that satisfy ECI. Then IRM is equivalent to minimizing $\sum_{e \in \mathcal{E}_{\text{tr}}} R_e(h \circ \phi)$ subject to $h \in \mathcal{F}, \phi \in \mathcal{G}_I$. Then by our theorem, the solution $\hat{h} \circ \hat{\phi}$ satisfies

$$R^{e_0}(\hat{h} \circ \hat{\phi}) \leq \sup_{e \in \mathcal{E}_{\text{tr}}} R^e(\hat{h} \circ \hat{\phi}) + \sup_{e, e' \in \mathcal{E}_{\text{tr}}} \mu_{\hat{\phi}}^{e, e'} + d_{\mathcal{G}_I}(e_0, \mathcal{E}_{\text{tr}}).$$

Compared to the original bound, ECI enforces perfect conditional label alignment, and also potentially reduces the generalization gap from $d_{\mathcal{G}}(e_0, \mathcal{E}_{\text{tr}})$ to $d_{\mathcal{G}_I}(e_0, \mathcal{E}_{\text{tr}})$ by pruning away those hypothesis ϕ that do not satisfy ECI on the sources. When the ground-truth indeed satisfies ECI, this will not hurt the sources risks and thus significantly decreases the bound on the target risk.

On the other hand, the last two terms in the bound imply two additional conditions for generalization. The covariate shift can be computed using the data from the sources, and thus can be incorporated into the training. The predictor adaptation gap is a condition on the target domain so it cannot be computed without target data, while it can be controlled by choosing proper hypothesis classes. We discuss these two terms in the following two subsections, respectively.

5.3 Representation Covariate Shift

Our analysis indicates a large representation distribution shift can lead to larger target risks, and only enforcing ECI will not suffice. Here we provide supporting empirical evidence, by experimenting on a variant of the colored MNIST dataset from [28]. The construction of the colored MNIST dataset is reviewed in Section 4, where the digit in the image is regarded as ground-truth representation. In the original construction, we have equal mass on the digits in both source domains, so there is no representation covariate shift. We modify the construction process so that the two source domains have *misaligned* distributions over the digits: e_1 has mass $\frac{p}{1+p}$ on digits 0-4 and $\frac{1}{1+p}$ on digits 5-9, while e_2 has mass $\frac{1}{1+p}$ on digits 0-4 and $\frac{p}{1+p}$ on digits 5-9. So the shift is controlled by a single control parameter p , as p increases the shift becomes larger. Figure 4 shows the results where p increases the test accuracy continues to decrease.⁵ The result demonstrates that as the representation covariate shift becomes more significant, models learned on the source domains have worse generalization to the test domain, which matches the implication of our analysis.

5.4 Predictor Adaptation Gap

When we find a model with low source risks and small conditional label divergence and covariate shift among the sources, can we guarantee that it has a low risk in the target domain? Our bound shows that this is not true when the

⁴ ECI and simultaneous optimality still have some subtle difference: When the loss does not have the property that the minimizer is the Bayesian optimal predictor, there are examples where simultaneous optimality does not enforce ECI. See Section C in the appendix for detailed discussions. Therefore, we use ECI for our analysis, since it is a property of the representation itself and does not involve the optimization and thus is more convenient for the analysis. On the other hand, simultaneous optimality is convenient for training.

⁵The exact data generating process is provided in Appendix D, and Table 1 there provides the detailed results.

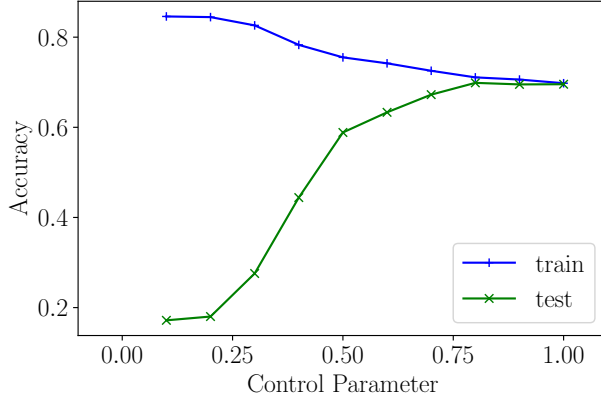


Figure 4: IRM under representation covariate shift. As the representation shift increases the test accuracy decreases. Note: the smaller the control parameter is, the larger the representation covariate shift is.

prediction adaptation gap $d_{\mathcal{G}_t}(e_0, \mathcal{E}_{tr})$ is large. When will the gap be large and lead to a high target risk? First, ECI is only imposed on the sources during training while it may not be satisfied in the target (i.e., a large conditional label divergence between the sources and the target), which can lead to a large gap. Second, even if all optimal solutions satisfy ECI in the target, some of them can have large representation covariate shift between the sources and the target, and thus still have a large target risk. (We emphasize that these are different from the conditional label divergence and the representation covariate shift among the sources, which can be controlled by the training algorithm.) We call these two cases *distribution memorization*. It is a phenomenon similar to overfitting via memorizing training samples in the traditional supervised learning setting, but it memorizes the entire distributions rather than the training samples. Even if infinite data from each source is available and the hypothesis classes are just slightly larger than necessary, distribution memorization can happen.

To demonstrate the distribution memorization phenomenon, here we give an intuitive example (due to the covariate shift between the sources and the target) and provide more in Section B.2. Consider the case with classification error, i.e., the label is in $\{-1, +1\}$ and the loss of f on data (x, y) is $\ell(f(x), y) = |\text{sign}(f(x)) - y|$. Suppose the support of the target $\text{supp}(X^{e_0})$ can be disjoint from those of the sources $\cup_{e \in \mathcal{E}_{tr}} \text{supp}(X^e)$. Assume: (1) There are ground-truth $\phi^* \in \mathcal{G}$ and $f^* \in \mathcal{F}$, such that $f^* \circ \phi^*$ has 0 error in all domains (including all sources and also the target), ϕ^* satisfies ECI in all domains, and the distributions of $\phi^*(X^e)$ are the same for all sources e . (2) The optimization finds f and ϕ such that in all sources, $f \circ \phi$ has 0 error, ϕ satisfies ECI, and the distributions of $\phi(X^e)$ are the same.

Proposition 1 (Distribution Memorization). *There exists an instance of the data distributions and $\mathcal{G} \circ \mathcal{F}$ satisfying the above assumptions, where there is an optimal solution $f \circ \phi$ that satisfies ECI and has 0 risks in all the source domains, but in the target domain has a risk 1/2 which is as large as random guessing. Furthermore, in the instance, $\phi(x)$ is simply the concatenation of $\phi^*(x)$ with one additional bit, and f is linear.*

Proof. Suppose the support of the target $\text{supp}(X^{e_0})$ can be disjoint from those of the sources $\cup_{e \in \mathcal{E}_{tr}} \text{supp}(X^e)$, and let $v(x) = 0$ if x is from a source $e \in \mathcal{E}_{tr}$ and $v(x) = 1$ if x is from the target e_0 . Suppose \mathcal{G} is large enough so that we have a $\phi \in \mathcal{G}$ that maps x to the concatenation of $\phi^*(x)$ and $v(x)$. Suppose f^* is linear and let \mathcal{F} be the set of linear functions, then we have an f with $f(\phi(x)) = f^*(\phi^*(x)) + 2v(x)$. Then for x from any source, $f(\phi(x)) = f^*(\phi^*(x))$, but for x from the target, $f(\phi(x)) = f^*(\phi^*(x)) + 2$. Suppose the target has an equal mass for the two class labels, then $h \circ \phi$ has source risks 0 but a large target risk 1/2. Furthermore, it is easy to see that in all sources, ϕ^* satisfies ECI and the distributions of $\phi^*(X^e)$ are the same. \square

Intuitively, the representation function remembers whether the data is from the target and then the predictor uses this to make different predictions for the target domain. More generally, we do not need the support of the target domain to be disjoint from those of the source domains. A similar phenomena can happen when the target has large total variation distances with the sources and the hypothesis classes are too large. Section B.2 provides an example where

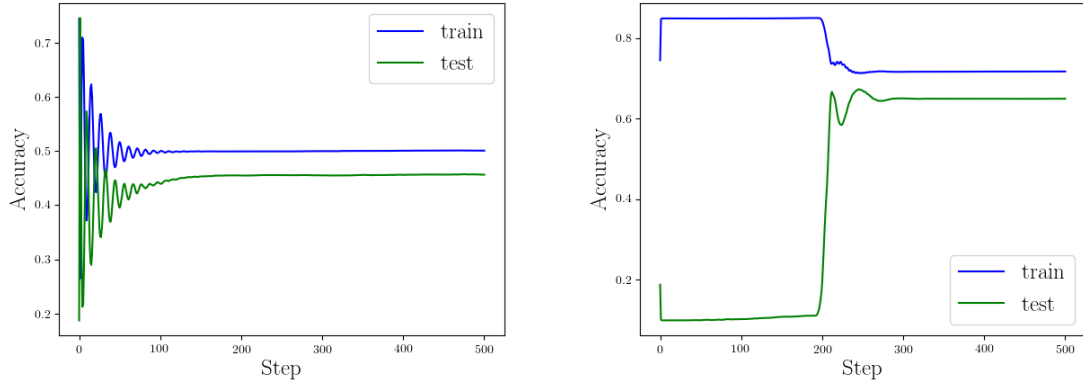


Figure 5: Training and test accuracy of IRMv1 v.s. epochs. Left: one-stage, use the regularization to impose ECI for the whole training. Right: two-stage, first train without the regularization for 190 steps and then use regularization.

the supports of the target and the sources overlap but a large representation covariate shift leads to a large gap. It also provides another example where the supports overlap while a large conditional label divergence leads to a large gap. The discussions thus suggest that with large hypothesis classes and a large difference between the sources and the target, we can have a large conditional label divergence and/or a large representation covariate shift between the sources and the target, which is reflected as a large prediction adaptation gap term in our bound.

Arguably, an interesting case for domain adaptation is when the target is significantly different from the sources, and our analysis shows that in this case, the hypothesis classes should be carefully chosen to alleviate the prediction adaptation gap and consequently get better generalization to the target domain. The connection between the prediction adaptation gap and the label divergence and covariate shift also suggests that if some (unlabeled) data from the target domain are available, such data can potentially be used to regularize the gap explicitly during the training.

Empirical evidence. [10] proposed an algorithm IRMv1 for IRM via regularization and evaluated it on the Color-MNIST dataset. We observe that, IRMv1 fails to learn on Color-MNIST when imposing the ECI regularization for the whole training process. The learned model has low source risks and small conditional label divergence and representation covariate shift, but has a high target risk indicating the existence of a large prediction adaptation gap. On the other hand, the algorithm succeeds with a two-stage training: First train without regularization, and then train with the regularization. Figure 5 gives the learning curves for the two training methods.

For this interesting observation, our analysis provides an explanation: the two-stage method is essentially pre-training, which reduces the size of the hypothesis classes and thus reduces the prediction adaptation gap. More precisely, the first stage begins with an initialization ϕ_0 and finds an intermediate solution ϕ_1 , and the second stage uses ϕ_1 as a warm start and searches in a neighborhood $\mathcal{N}(\phi_1)$ of ϕ_1 to obtain the final solution ϕ_2 . Here, $\mathcal{N}(\phi_1)$ can be much smaller than the original hypothesis class \mathcal{G}_I . Then the predictor adaptation gap reduces from $d_{\mathcal{G}_I}(e_0, \mathcal{E}_{tr})$ to $d_{\mathcal{N}(\phi_1)}(e_0, \mathcal{E}_{tr})$, and thus improves generalization. This explanation can be verified empirically. We computed the ℓ_2 distance between the parameters of ϕ_0 and ϕ_1 , and for ϕ_1 and ϕ_2 . The latter is less than 8% of the former, suggesting that it is indeed doing pre-training and supporting our explanation. This also suggests that the two-stage training heuristic can be a general strategy in future algorithm design to improve generalization to the target domain.

6 Discussions

It is instructive to compare our results for single-source and multi-source environment. The risk bound for multi-source case has an additional term (the predictor adaptation distance). This is because we intentionally separate the quantities that can be optimized on the sources (i.e., the source risks, the conditional label divergence, and the covariate shift), and those that are related to the target and thus cannot be optimized in the setting without data from the target (the predictor adaptation distance). Separating out the second part helps to identify conditions of the target for generalization. In

the single-source case, both the label divergence and the covariate shift are related to the target domain so we do not separate the two parts. This also means that directly applying Theorem 1 to the multi-source setting leads to a bound using conditional label divergence and covariate shift between the target and the sources. This does not provide insights about the multi-source setting and explanations for the examples we considered in Section 5.

We further comment that our bounds are finer-grained than the classic bounds for domain adaptation based on \mathcal{H} -divergence, e.g., that by [13]. For single source, a similar bound as Theorem 1 can be derived from the classic \mathcal{H} -divergence based bound, by bounding the \mathcal{H} -divergence by the label divergence and covariate shift. On the other hand, the bound in Theorem 1 is tighter (it is an *equality*!) and the analysis is more intuitive. For multiple sources, we can also derive a multi-source \mathcal{H} -divergence based bound. Our multi-source bound can also be viewed as decomposing the \mathcal{H} -divergence into finer-grained quantities. See Section E in the appendix for the details.

7 Conclusions

We presented risk bounds for learning invariant representations across domains, based on new decompositions specific for representation learning. It allows us to identify the conditions for successful invariant representation learning. In particular, we use them to investigate several interesting failure examples of existing approaches such as DANN and IRM, revealing that the regularizations in these approaches are complementary. Our risk bounds show that explicitly incorporating representations can provide novel implications, and open an avenue for designing future algorithms for representation learning in domain adaptation.

References

- [1] S. Ben-David, J. Blitzer, K. Crammer, and F. Pereira, “Analysis of representations for domain adaptation,” in *Advances in Neural Information Processing Systems 19, Proceedings of the Twentieth Annual Conference on Neural Information Processing Systems, Vancouver, British Columbia, Canada, December 4-7, 2006*, B. Schölkopf, J. C. Platt, and T. Hofmann, Eds. MIT Press, 2006, pp. 137–144.
- [2] Y. Ganin, E. Ustinova, H. Ajakan, P. Germain, H. Larochelle, F. Laviolette, M. Marchand, and V. S. Lempitsky, “Domain-adversarial training of neural networks,” in *Domain Adaptation in Computer Vision Applications*, ser. Advances in Computer Vision and Pattern Recognition, 2017, pp. 189–209.
- [3] F. D. Johansson, D. A. Sontag, and R. Ranganath, “Support and invertibility in domain-invariant representations,” in *The 22nd International Conference on Artificial Intelligence and Statistics, AISTATS 2019, 16-18 April 2019, Naha, Okinawa, Japan*, 2019, pp. 527–536.
- [4] Y. Bengio, A. Courville, and P. Vincent, “Representation learning: A review and new perspectives,” *IEEE transactions on pattern analysis and machine intelligence*, vol. 35, no. 8, pp. 1798–1828, 2013.
- [5] O. Sener, H. O. Song, A. Saxena, and S. Savarese, “Learning transferrable representations for unsupervised domain adaptation,” in *Advances in Neural Information Processing Systems*, 2016, pp. 2110–2118.
- [6] A. Dosovitskiy and T. Brox, “Inverting visual representations with convolutional networks,” in *Proceedings of the IEEE conference on computer vision and pattern recognition*, 2016, pp. 4829–4837.
- [7] J. Devlin, M.-W. Chang, K. Lee, and K. Toutanova, “Bert: Pre-training of deep bidirectional transformers for language understanding,” *arXiv preprint arXiv:1810.04805*, 2018.
- [8] M. E. Peters, M. Neumann, M. Iyyer, M. Gardner, C. Clark, K. Lee, and L. Zettlemoyer, “Deep contextualized word representations,” *arXiv preprint arXiv:1802.05365*, 2018.
- [9] H. Zhao, R. T. des Combes, K. Zhang, and G. J. Gordon, “On learning invariant representations for domain adaptation,” in *Proceedings of the 36th International Conference on Machine Learning, ICML 2019, 9-15 June 2019, Long Beach, California, USA*, 2019, pp. 7523–7532.

- [10] M. Arjovsky, L. Bottou, I. Gulrajani, and D. Lopez-Paz, “Invariant risk minimization,” *CoRR*, vol. abs/1907.02893, 2019.
- [11] D. Kifer, S. Ben-David, and J. Gehrke, “Detecting change in data streams,” in *VLDB*, vol. 4. Toronto, Canada, 2004, pp. 180–191.
- [12] J. Blitzer, K. Crammer, A. Kulesza, F. Pereira, and J. Wortman, “Learning bounds for domain adaptation,” in *Advances in neural information processing systems*, 2008, pp. 129–136.
- [13] S. Ben-David, J. Blitzer, K. Crammer, A. Kulesza, F. Pereira, and J. W. Vaughan, “A theory of learning from different domains,” *Machine learning*, vol. 79, no. 1-2, pp. 151–175, 2010.
- [14] H. Ajakan, P. Germain, H. Larochelle, F. Laviolette, and M. Marchand, “Domain-adversarial neural networks,” *stat*, vol. 1050, p. 15, 2014.
- [15] Y. Ganin, E. Ustinova, H. Ajakan, P. Germain, H. Larochelle, F. Laviolette, M. Marchand, and V. Lempitsky, “Domain-adversarial training of neural networks,” *The Journal of Machine Learning Research*, vol. 17, no. 1, pp. 2096–2030, 2016.
- [16] Z. Pei, Z. Cao, M. Long, and J. Wang, “Multi-adversarial domain adaptation,” in *Thirty-Second AAAI Conference on Artificial Intelligence*, 2018.
- [17] H. Zhao, S. Zhang, G. Wu, J. M. Moura, J. P. Costeira, and G. J. Gordon, “Adversarial multiple source domain adaptation,” in *Advances in neural information processing systems*, 2018, pp. 8559–8570.
- [18] H. Zhao, S. Zhang, G. Wu, G. J. Gordon *et al.*, “Multiple source domain adaptation with adversarial learning,” in *ICLR*, 2018.
- [19] M. Long, J. Wang, G. Ding, J. Sun, and P. S. Yu, “Transfer joint matching for unsupervised domain adaptation,” in *Proceedings of the IEEE conference on computer vision and pattern recognition*, 2014, pp. 1410–1417.
- [20] M. Long, Y. Cao, J. Wang, and M. I. Jordan, “Learning transferable features with deep adaptation networks,” *arXiv preprint arXiv:1502.02791*, 2015.
- [21] N. Courty, R. Flamary, A. Habrard, and A. Rakotomamonjy, “Joint distribution optimal transportation for domain adaptation,” in *Advances in Neural Information Processing Systems*, 2017, pp. 3730–3739.
- [22] J. Shen, Y. Qu, W. Zhang, and Y. Yu, “Wasserstein distance guided representation learning for domain adaptation,” in *Thirty-Second AAAI Conference on Artificial Intelligence*, 2018.
- [23] Y. Mansour, M. Mohri, and A. Rostamizadeh, “Multiple source adaptation and the rényi divergence,” in *Proceedings of the Twenty-Fifth Conference on Uncertainty in Artificial Intelligence*, 2009, pp. 367–374.
- [24] K. Zhang, B. Schölkopf, K. Muandet, and Z. Wang, “Domain adaptation under target and conditional shift,” in *International Conference on Machine Learning*, 2013, pp. 819–827.
- [25] M. Gong, K. Zhang, T. Liu, D. Tao, C. Glymour, and B. Schölkopf, “Domain adaptation with conditional transferable components,” in *International conference on machine learning*, 2016, pp. 2839–2848.
- [26] K. Azizzadenesheli, A. Liu, F. Yang, and A. Anandkumar, “Regularized learning for domain adaptation under label shifts,” *arXiv preprint arXiv:1903.09734*, 2019.
- [27] H. Zhao, R. T. Des Combes, K. Zhang, and G. Gordon, “On learning invariant representations for domain adaptation,” in *International Conference on Machine Learning*, 2019, pp. 7523–7532.
- [28] M. Arjovsky, L. Bottou, I. Gulrajani, and D. Lopez-Paz, “Invariant risk minimization,” *arXiv preprint arXiv:1907.02893*, 2019.

- [29] Y. Li, X. Tian, M. Gong, Y. Liu, T. Liu, K. Zhang, and D. Tao, “Deep domain generalization via conditional invariant adversarial networks,” in *Computer Vision - ECCV 2018 - 15th European Conference, Munich, Germany, September 8-14, 2018, Proceedings, Part XV*, ser. Lecture Notes in Computer Science, vol. 11219. Springer, 2018, pp. 647–663.
- [30] J. Peters, P. Bühlmann, and N. Meinshausen, “Causal inference using invariant prediction: identification and confidence intervals,” *arXiv e-prints*, p. arXiv:1501.01332, Jan 2015.
- [31] S. J. Pan, I. W. Tsang, J. T. Kwok, and Q. Yang, “Domain adaptation via transfer component analysis,” *IEEE Transactions on Neural Networks*, vol. 22, no. 2, pp. 199–210, 2010.

A Proofs for Section 4

A.1 Group Fairness Bound for Covariate Shift

Let \mathcal{B} be a partition of the space of the representation ϕ . Assume for simplicity $|\mathcal{B}|$ is finite.

Definition 9 (Group Representation Source Fairness). *The group (representation) source fairness $\rho_{\phi, \mathcal{B}}^s$ with respect to \mathcal{B} is defined as $\rho_{\phi, \mathcal{B}}^s := \sup_{B \in \mathcal{B}'} \{H(Y^s | \Phi^s \in B)\}$, where $\mathcal{B}' = \{B \in \mathcal{B} : \Pr[\Phi^s \in B] > 0\}.$*

Definition 10 (Group Distance). *The group distance between two distributions μ and ν with respect to \mathcal{B} is defined as $d_{\mathcal{B}}(\mu, \nu) = \frac{1}{2} \sum_{B \in \mathcal{B}} |\mu(B) - \nu(B)|$.*

Corollary 2. *Suppose Φ^t is supported on Φ^s , i.e., if $\Pr[\Phi^t \in B] > 0$ for some set B , then $\Pr[\Phi^s \in B] > 0$. Then we have*

$$\begin{aligned} \mu_{\phi}^{s,t} &\leq \rho_{\phi, \mathcal{B}}^s \times d_{\mathcal{B}}(\Phi^s, \Phi^t) \\ &\leq \rho_{\phi}^s \times d_{\text{TV}}(\Phi^s, \Phi^t) \\ &\leq \log K \times d_{\text{TV}}(\Phi^s, \Phi^t). \end{aligned}$$

Proof. We have

$$\begin{aligned} \mu_{\phi}^{s,t} &= \int_{\Omega} H(Y^s | \gamma^s) \mu^t(d\gamma) - \int_{\Omega} H(Y^s | \gamma^s) \mu^s(d\gamma) \\ &= \sum_{B \in \mathcal{B}'} \Pr[\Phi^t \in B] H(Y^s | \Phi^s \in B) - \sum_{B \in \mathcal{B}'} \Pr[\Phi^s \in B] H(Y^s | \Phi^s \in B) \\ &= \sum_{B \in \mathcal{B}'} (\Pr[\Phi^t \in B] - \Pr[\Phi^s \in B]) H(Y^s | \Phi^s \in B) \\ &\leq \sum_{B \in \mathcal{B}'} \max \{0, \Pr[\Phi^t \in B] - \Pr[\Phi^s \in B]\} H(Y^s | \Phi^s \in B) \\ &\leq \sup_{B \in \mathcal{B}'} H(Y^s | \Phi^s \in B) \times \sum_{B \in \mathcal{B}'} \max \{0, \Pr[\Phi^t \in B] - \Pr[\Phi^s \in B]\} \\ &= \sup_{B \in \mathcal{B}'} H(Y^s | \Phi^s \in B) \times \frac{1}{2} \sum_{B \in \mathcal{B}'} |\Pr[\Phi^t \in B] - \Pr[\Phi^s \in B]| \\ &\leq \rho_{\phi, \mathcal{B}}^s \times d_{\mathcal{B}}(\Phi^s, \Phi^t). \end{aligned}$$

Clearly, $\rho_{\phi, \mathcal{B}}^s \leq \rho_{\phi}^s$. Let $U(\mathcal{B})$ be the family of sets that can be obtained by taking union of some sets in \mathcal{B} :

$$U(\mathcal{B}) = \{U : U = \cup_{B \in \mathcal{B}} B, \mathcal{A} \subseteq \mathcal{B}\}.$$

Then $d_{\mathcal{B}}(\mu, \nu) = \sup_{U \in U(\mathcal{B})} |\mu(U) - \nu(U)| \leq d_{\text{TV}}(\mu, \nu)$, where the last inequality follows from the definition of total variation distance. So the statement follows. \square

B Proofs in Section 5

B.1 Proof of Theorem 2

For any $e \in \mathcal{E}_{\text{tr}}$,

$$\begin{aligned} &R^{e_0}(f_{\phi}^e \circ \phi) - R^e(f_{\phi}^e \circ \phi) \\ &= \inf_{e' \in \mathcal{E}_{\text{tr}}} [R^{e_0}(f_{\phi}^e \circ \phi) - R^{e'}(f_{\phi}^e \circ \phi) + R^{e'}(f_{\phi}^e \circ \phi) - R^e(f_{\phi}^e \circ \phi)] \\ &\leq \inf_{e' \in \mathcal{E}_{\text{tr}}} [R^{e_0}(f_{\phi}^e \circ \phi) - R^{e'}(f_{\phi}^e \circ \phi)] + \sup_{e' \in \mathcal{E}_{\text{tr}}} [R^{e'}(f_{\phi}^e \circ \phi) - R^e(f_{\phi}^e \circ \phi)]. \end{aligned}$$

Therefore, taking $\sup_{e \in \mathcal{E}_{\text{tr}}}$ on both sides and applying the max-min inequality leads to

$$\sup_{e \in \mathcal{E}_{\text{tr}}} R^{e_0}(f_\phi^e \circ \phi) \leq \sup_{e \in \mathcal{E}_{\text{tr}}} R^e(f_\phi^e \circ \phi) + d_\phi(e_0, \mathcal{E}_{\text{tr}}) + \sup_{e, e' \in \mathcal{E}_{\text{tr}}} [R^{e'}(f_\phi^e \circ \phi) - R^e(f_\phi^e \circ \phi)].$$

For the last term, using the same argument as in Theorem 1,

$$R^{e'}(f_\phi^e \circ \phi) - R^e(f_\phi^e \circ \phi) = \delta_\phi^{e, e'} + \text{KL}_\phi^{e, e'} + \mu_\phi^{e, e'}.$$

This completes the proof.

B.2 Distribution Memorization under Milder Assumptions

Proposition 1 shows large hypothesis classes can lead to too large predictor adaptation gap, but assuming the support of the target is disjoint with those of the sources. Here we show that this assumption is not needed in general, but just for the simplicity of the presentation and illustration of intuition.

Consider the following example. The input x lies on the real line. The conditional probability of the label $Y|X$ are the same for all domains: $Y = 0$ on $[-2, -1] \cup [1, 2]$, $Y = 1$ on $[-1, 1]$, and $\Pr[Y = 0|x] = \Pr[Y = 1|x] = 1/2$ for any $x \in [2, 3]$. The distributions of X are specified as follows.

1. The target domain e_0 puts uniformly mass ϵ on the interval $[-2, 0]$, mass ϵ on $[0, 2]$, and mass $1 - 2\epsilon$ on $[2, 3]$.
2. Source e_1 puts uniformly mass $1 - 2\epsilon$ on the interval $[-2, 0]$, mass ϵ on $[0, 2]$, and mass ϵ on $[2, 3]$.
3. Source e_2 puts mass ϵ on the interval $[-2, 0]$, mass $1 - 2\epsilon$ on $[0, 2]$, and mass ϵ on $[2, 3]$.

Then $\phi(x) = |x|$ and the classifier $f(\phi(x)) = \mathbf{1}[\phi(x) \leq 1]$ have the optimal error and satisfy ECI on the sources, but still has a large error $(1 - 2\epsilon)/2$ in the target domain. This is reflected by a large predictor adaptation gap. In this particular example, the gap is due to the covariate shift between the sources and the target (similar to the example in Proposition 1).

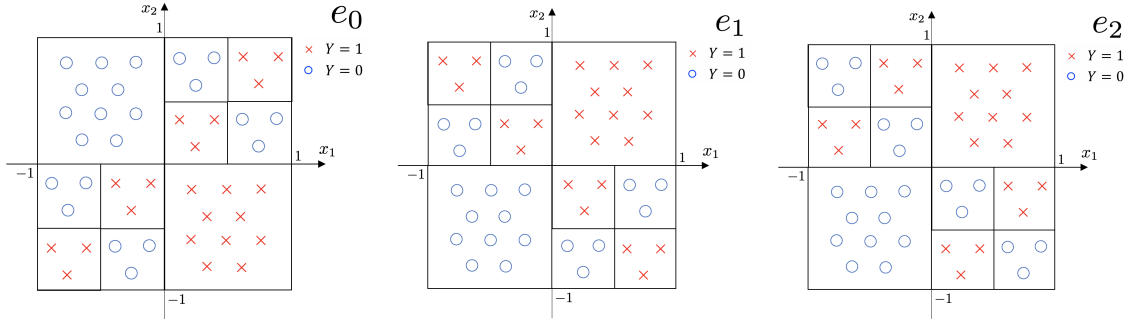


Figure 6: Illustrating example of distribution memorization: e_1 and e_2 are the two source environments, e_0 is the target environment. Both $\phi_1(x) = x_1$ and $\phi_2(x) = x_2$ satisfy the source ECI and zero source covariate shift. However, ϕ_2 will lead to a large target error.

Consider another example, shown in Figure 6. It is a variant of Example 1. The input space $\mathcal{X} = [-1, 1] \times [-1, 1]$, $\mathcal{G} = \{\phi_1, \phi_2\}$ where $\phi_1(x) = x_1$ and $\phi_2(x) = x_2$, and $\mathcal{F} = \{\mathbf{1}_\lambda(\cdot)\}$ (that is we consider thresholding functions that $\mathbf{1}_\lambda(\alpha) = 1$ if $\alpha > \lambda$, and 0 otherwise). The distributions are specified as follows. Let $\epsilon > 0$ be a sufficiently small constant.

1. The target e_0 puts uniformly mass $1/2 - \epsilon$ in the second and fourth quadrants, and mass ϵ in the first and third quadrants. It has label 1 for the fourth quadrant and label 0 for the second quadrant. In the first and third quadrant, it has label 1 for points in $[-1, -1/2] \times [-1, -1/2]$ or $[-1/2, 0] \times [-1/2, 0]$ or $[0, 1/2] \times [0, 1/2]$ or $[1/2, 1] \times [1/2, 1]$, and has label 0 for the other points.

2. Source e_1 puts uniformly mass $1/2 - \epsilon$ in the first and third quadrants, and mass ϵ in the second and fourth quadrants. It has label 1 for the first quadrant and label 0 for the third quadrant. In the second and fourth quadrant, it has label 1 for points in $[-1, -1/2] \times [1/2, 1]$ or $[-1/2, 0] \times [0, 1/2]$ or $[0, 1/2] \times [-1/2, 0]$ or $[1/2, 1] \times [-1, -1/2]$, and has label 0 for the other points.
3. Source e_2 puts uniformly mass $1/2 - \epsilon$ in the first and third quadrants, and mass ϵ in the second and fourth quadrants. It has label 1 for the first quadrant and label 0 for the third quadrant. In the second and fourth quadrant, it has label 0 for points in $[-1, -1/2] \times [1/2, 1]$ or $[-1/2, 0] \times [0, 1/2]$ or $[0, 1/2] \times [-1/2, 0]$ or $[1/2, 1] \times [-1, -1/2]$, and has label 1 for the other points.

So both ϕ_1 and ϕ_2 lead to the optimal error and satisfy ECI in the sources. But ϕ_1 and the corresponding classifier $\mathbf{1}_0(\cdot)$ lead to a small error ϵ in the target, while ϕ_2 and the corresponding classifier $\mathbf{1}_0(\cdot)$ lead to a large error $1 - \epsilon$ in the target. Again, this is reflected by a large predictor adaptation gap. But in this particular example, the gap is due to the representation conditional label misalignment between the sources and the target.

In summary, both the representation conditional label misalignment and the covariate shift between the sources and the target can lead to a large predictor adaptation gap and consequently a large generalization gap, even when we can make sure the representation conditional label misalignment and the covariate shift among the sources are small. The precise relationship between the predictor adaptation gap and the misalignment/covariate shift between the sources and the target is left for future work.

C Relationship between ECI and IRM

Recall that the IRM approach proposed by [10] is to find $\hat{h}, \hat{\phi}$ by:

$$\min_{h \in \mathcal{F}, \phi \in \mathcal{G}} \sum_{e \in \mathcal{E}_{\text{tr}}} R^e(h \circ \phi), \quad (2)$$

$$\text{subject to } h \in \arg \min_{h \in \mathcal{F}} R^e(h \circ \phi) \text{ for any } e \in \mathcal{E}_{\text{tr}}. \quad (3)$$

This is empirical risk minimization subject to *simultaneous optimality* of the predictor for all sources. As pointed in [10], when the loss has the property that the minimizer is the Bayesian optimal predictor and \mathcal{F} is large enough to include that, ECI and simultaneous optimality are equivalent. Specifically we consider the following definition:

Definition 11 (ϕ -Bayesian Optimality Property). Let $\phi : X \mapsto \mathcal{R}$ be a representation, $\ell : \Delta_K \times [K] \mapsto \mathbb{R}^+$ be a loss function, where $\Delta_K = \{(p_1, \dots, p_K) \mid p_i \geq 0, \sum_{i=1}^K p_i = 1\}$ is the K -dimensional probability simplex. Consider the following optimization problem:

$$\underset{w: \mathcal{R} \mapsto \Delta_K}{\text{minimize}} \quad \mathbb{E}[\ell(f(\phi(X)), Y)] \quad (4)$$

where the expectation is taken over X, Y . We say that ℓ has the Bayesian optimality property with respect to ϕ , if the optimal solution $f^* : \mathcal{R} \mapsto \Delta_K$ of (4), which maps a representation to a probability vector, satisfies that

$$\forall \gamma \in \text{supp}(\Phi), \forall y \in [K] : f^*(\gamma)_y = \Pr[Y = y \mid \Phi = \gamma]$$

Note that the simultaneous optimality is required for some $h \in \mathcal{F}$, while ECI or invariant predictor doesn't require h to be from \mathcal{F} . When the loss function has the Bayesian optimality property, ϕ satisfying ECI is equivalent to ϕ eliciting an invariant predictor (see the discussion later). We prefer to center our analysis around ECI rather than invariant predictor or simultaneous optimality for convenience, while simultaneous optimality is very useful for enforcing ECI in training.

Here, we analyze IRM under the following assumptions:

- (A1) The loss has the Bayesian optimality property.
- (A2) \mathcal{F} is sufficiently large to include the conditional probabilities $g(r) = \Pr(Y^e \mid \phi(X^e) = r)$ for any $\phi \in \mathcal{G}$ and any $e \in \mathcal{E}_{\text{tr}} \cup \{e_0\}$.

Under (A1)(A2), simultaneous optimality is equivalent to ϕ satisfying ECI.

It is worth noting many natural loss functions (e.g. squared loss, cross entropy) satisfies Bayesian optimality property. Combining (A1) and (A2), we have the following proposition:

Proposition 2. *Let ϕ be a representation, ℓ be a loss function that satisfies the Bayesian optimality property w.r.t. ϕ , and \mathcal{E} be an environment family. Suppose that ϕ is conditionally invariant w.r.t. \mathcal{E} . Assuming (A2), then there is a universal optimal solution $f_\phi \in \mathcal{F}$ to the optimization problem $\min_h \mathbb{E}[\ell(h(\phi(X^e), Y^e))]$ across all $e \in \mathcal{E}$.*

Proof. Define f_ϕ as

$$[f_\phi(r)]_y := [f_\phi^e(r)]_y = \Pr[Y^e = y \mid \phi(X^e) = r], y \in [K] \quad \text{for any } e \in \mathcal{E} \text{ that } \phi \in \text{supp}(\phi(X^e))$$

We note that f_ϕ is consistently defined because ϕ is conditionally invariant w.r.t. \mathcal{E} . Clearly, f_ϕ is optimal because ℓ satisfies Bayesian optimality property. \square

Now, given an environment family \mathcal{E} , and (A1) (A2) satisfied, by Proposition 2, we can consider the following objective:

$$\begin{aligned} & \underset{\phi}{\text{minimize}} \quad \sum_{e \in \mathcal{E}} \mathbb{E}[\ell(f_\phi(\phi(X^e)), Y^e)] \\ & \text{subject to ECI}(\phi, \mathcal{E}) \end{aligned} \tag{ERM-ECI}$$

Proposition 3. (ERM-ECI) is exactly the (IRM) objective defined as

$$\begin{aligned} & \underset{h, \phi}{\text{minimize}} \quad \sum_{e \in \mathcal{E}} \mathbb{E}[\ell(h(\phi(X^e)), Y^e)] \\ & \text{subject to } (\forall e \in \mathcal{E}) h \in \arg \min_{\bar{h}} \mathbb{E}[\ell(\bar{h}(\phi(X^e)), Y^e)] \end{aligned} \tag{IRM}$$

Proof. Because ℓ satisfies the conditional expectation property, therefore we know that for every $e \in \mathcal{E}$ the optimal solution will output the optimal conditional probability. Therefore for (IRM), the only possibility that there is an invariant optimal solution h across all environments, is that ϕ is conditionally invariant w.r.t. \mathcal{E} . However, then we know that the invariant optimal solution h in (IRM) is nothing but the f_ϕ . The proof is complete. \square

Without (A1)(A2), simultaneous optimality may not impose ECI; see an example in the next subsection.

C.1 Example Showing the Difference of ECI and IRM

C.1.1 Review of the colored-MNIST Experiment

In the paper [10], an interesting experiment on colored-MNIST is performed. The experiment is essentially as follows:

1. We start by considering a random variable G which encodes digits. Specifically, G is a random variable on \mathbb{R}^d of pixels. We abuse the notation to use G to denote the true digit its pixels encode (e.g. $G = 0$ means a sample that encodes 0).
2. We then define a Bernoulli random variable X as

$$X = \begin{cases} 0 & \text{if } G = 0, 1, 2, 3, 4, \\ 1 & \text{if } G = 5, 6, 7, 8, 9 \end{cases}$$

In other words, $X = 0$ if the digit encoded in G is less than 5, and 1 otherwise.

3. The *true label* Y is generated by flipping X with probability .25. That is,

$$Y = \begin{cases} X & \text{w.p. .75,} \\ 1 - X & \text{w.p. .25} \end{cases}$$

In other words, the predictability⁶ of Y using X is $\Pr[X = Y] = .75$.

4. Then we create a *color random variable* Z , by flipping Y with probability q (define $p = 1 - q$). That is,

$$Z = \begin{cases} Y & \text{w.p. } p, \\ 1 - Y & \text{w.p. } q \end{cases}$$

That is, the predictability of Y using Z is p if $p > 1/2$, and q if $p \leq 1/2$.

5. Finally, after the color Z is sampled, we create a new pixel random variable \tilde{G} , by coloring the pixels of the digit in G using color Z (red if $Z = 0$ and green if $Z = 1$). Clearly, the causal structure is



Correlation between Y and Z is variant and thus is spurious. Note that both x and z can be recovered from \tilde{g} .

6. The task is to train a classifier to *predict* Y from \tilde{G} (that is a model $\tilde{G} \mapsto Y$). The experiment in [10] defines three environments: **(e₁)** where $q = .1$, which generates Z^{e_1} . Note that $\Pr[Y = Z^{e_1}] = .9 > .75 = \Pr[X = Y]$. **(e₂)** where $q = .2$, which generates Z^{e_2} . Note that $\Pr[Y = Z^{e_2}] = .8 > .75 = \Pr[X = Y]$. **(e₃)** (test environment): where $q = .9$, which generates Z^{e_3} . Note that now $\Pr[Y = Z^{e_3}] = .1 \ll .75 = \Pr[X = Y]$. That is, while in training environments Z is highly predictive, in the test environment it is poorly performing (and instead it is $1 - Z$ that is highly predictive).

IRM paper uses e_1 and e_2 for training. It is straightforward now to instantiate both (IRM) and (IRMv1) objectives with the above setting. Interestingly, with (IRMv1), [10] found that they can learn to use X , but not Z . In a nutshell, they claim that, even with the following two assumptions:

1. The correlation between Y and Z *varies* over training environments.
2. In every training environment Z is more predictive than X in predicting Y .

IRM can still learn *not* to use correlations that are *not* invariant.

C.1.2 Example where IRM Does Not Impose ECI

We now prove that if we use the 0-1 loss (which does not have the Bayesian optimality property), then the optimal solutions to (IRM) in color-MNIST do not satisfy ECI and should learn the spurious correlation Z (i.e., the color).

To start with, we consider 0-1 loss, that is, given hypothesis h that maps $g \sim \tilde{G}$ to $\{0, 1\}$,

$$\ell(g, y; h) = \mathbb{1}[h(g) \neq y] = \begin{cases} 1 & h(g) \neq y, \\ 0 & \text{otherwise.} \end{cases}$$

and therefore $R^e(h)$ is defined to be $\sum_{(g,y) \sim \tilde{G}^e} \ell(g, y; h)$.

Our construction has two steps: First, we construct one optimal solution (Φ^*, w^*) to (IRM), but which learns the spurious correlation Z . Second, we prove that *any* optimal solution should learn the spurious correlation Z .

Constructing an optimal (Φ^*, w^*) to (IRM). Now, we construct representation Φ^* and classifier w^* :

⁶ We define the *predictability* of a binary random variable Y using another binary random variable X as $\max\{\Pr[Y = X], \Pr[Y = 1 - X]\}$.

- We let Φ^* be the representation that maps a colored image $g \sim \tilde{G}$ to a binary vector in $\{0, 1\}^2$:

$$\Phi^*(\tilde{G}) = \begin{bmatrix} X \\ Z \end{bmatrix}$$

That is, from \tilde{G} , Φ^* optimally reconstructs the digit concept X and color concept Z .

- We construct classifier w^* as

$$w^* = \begin{bmatrix} 0 \\ 1 \end{bmatrix}$$

In other words, $(w^*)^\top \Phi^*(\tilde{G}) = Z$, which simply outputs the color concept.

We have the following proposition,

Proposition 4. *For 0-1 loss, (Φ^*, w^*) is an optimal solution to (IRM). Specifically, outputting color Z using w^* is optimal in e_1 and e_2 respectively, and achieves minimal empirical risk combining environments e_1 and e_2 .*

Proof. Consider the Bayesian optimal classifier c^* given X, Z . That is

$$c^*(x, z) = \begin{cases} 1 & \text{if } \Pr[Y = 1|x, z] > 1/2 \\ 0 & \text{otherwise.} \end{cases}$$

For any predictor $f : \tilde{G} \mapsto \{0, 1\}$, we show that $\Pr[Y \neq f(\tilde{G})] \geq \Pr[Y \neq c^*(X, Z)]$. That is $c^*(X, Z)$ achieves the optimal error among all predictors over \tilde{G} . To see this, note that from (Causal Structure), we have that $Y \perp\!\!\!\perp \tilde{G} \mid (X, Z)$. Thus $Y \perp\!\!\!\perp f(\tilde{G}) \mid (X, Z)$. Therefore by the law of total expectation

$$\begin{aligned} \Pr[Y \neq f(\tilde{G})] &= \mathbb{E}_{X, Z} [\mathbb{E}[\mathbb{1}\{Y \neq f(\tilde{G})\} \mid X, Z]] \\ &= \sum_{x, z} p(x, z) \cdot \left(p(Y = 1, f(\tilde{G}) = 0 \mid x, z) + p(Y = 0, f(\tilde{G}) = 1 \mid x, z) \right) \\ &= \sum_{x, z} p(x, z) \cdot \left(p(Y = 1 \mid x, z) p(f(\tilde{G}) = 0 \mid x, z) + p(Y = 0 \mid x, z) p(f(\tilde{G}) = 1 \mid x, z) \right) \\ &\geq \sum_{x, z} p(x, z) \cdot \min \left\{ p(Y = 1 \mid x, z), p(Y = 0 \mid x, z) \right\} \\ &= \sum_{x, z} p(x, z) \cdot \Pr[Y \neq c^*(x, z)] \\ &= \Pr[Y \neq c^*(X, Z)] \end{aligned}$$

Clearly, $\Phi^*(\tilde{G}) = (X, Z)$. Next we show that $c^* = w^*$. For each environment we can compute the Bayesian optimal predictor $\Pr[Y = y \mid X = x, Z = z]$, for $x, y, z \in \{0, 1\}$. We have that,

| e₁ | $y = 0$ | $y = 1$ | e₂ | $y = 0$ | $y = 1$ |
|----------------------|-----------------------------------|-----------------------------------|----------------------|-----------------------------------|-----------------------------------|
| $x = 0, z = 0$ | $\frac{27}{28}$ | $\frac{1}{28}$ | $x = 0, z = 0$ | $\frac{12}{13}$ | $\frac{1}{13}$ |
| $x = 0, z = 1$ | $\frac{1}{4}$ | $\frac{3}{4}$ | $x = 0, z = 1$ | $\frac{3}{7}$ | $\frac{4}{7}$ |
| $x = 1, z = 0$ | $\frac{3}{4}$ | $\frac{1}{4}$ | $x = 1, z = 0$ | $\frac{4}{7}$ | $\frac{3}{7}$ |
| $x = 1, z = 1$ | $\frac{1}{28}$ | $\frac{27}{28}$ | $x = 1, z = 1$ | $\frac{1}{13}$ | $\frac{12}{13}$ |

For each row, we highlight (bold) the cell which Bayesian optimal predictor should output. One can see that for either environment, the Bayesian optimal predictor is simply to output z . This shows that:

- z is the optimal predictor for e_1 and e_2 , respectively, and,
- The Bayesian optimal predictor for e_1 and e_2 together is also simply z .

We note that $w^* \circ \Phi^*$ gives the optimal predictor z , and also that w^* is the optimal hypothesis for $\Phi^*(\tilde{G}^{e_1})$ and $\Phi^*(\tilde{G}^{e_2})$, respectively. Therefore (w^*, Φ^*) is an optimal solution to (IRM). \square

From “an” optimal solution to “any” optimal solution. We have the following:

Proposition 5. *For 0-1 loss, and any optimal solution $\bar{\Phi}, \bar{w}$ to (IRM), $\bar{w} \circ \bar{\Phi}$ must be Z (i.e., the color).*

Proof. Consider any optimal solution $\bar{\Phi}$ and \bar{w} to (IRM). It must satisfy that its empirical loss across all environments must be upper bounded by that of Φ^* and w^* . That is,

$$R^{e_1}(\bar{w} \circ \bar{\Phi}) + R^{e_2}(\bar{w} \circ \bar{\Phi}) \leq R^{e_1}(w^* \circ \Phi^*) + R^{e_2}(w^* \circ \Phi^*).$$

However $w^* \circ \Phi^*$ is the Bayesian optimal predictor Z . This means that $\bar{w} \circ \bar{\Phi}$ must also be Z . The proof is complete. \square

Combining Propositions 4 and 5 it shows that (IRM) cannot impose ECI and learn invariant correlations.

D Experimental Details for IRM under Representation Covariate Shift

There are two training environments e_1, e_2 and one testing environment e_0 . The data is generated with two control parameter p, n as follows: We first we assign a preliminary label $\tilde{y} = 0$ for digit 0 – 4, and $\tilde{y} = 1$ for digit 5 – 9 for each data point in MNIST. Then to create e_1, e_2 , we randomly partition the 50000 MNIST training samples into two sets S_1 and S_2 . In e_1 , we sample n points with replacement from set S_1 to obtain data from 0-4 with probability $\frac{p}{1+p}$ and data from 5-9 with probability $\frac{1}{1+p}$; in e_2 , we sample n points with replacement from set S_2 to obtain data from 0-4 with probability $\frac{1}{1+p}$ and data from 5-9 with probability $\frac{p}{1+p}$. Finally, we create final label (true label) for data in all environments, y , by flipping \tilde{y} with probability 0.25. Finally, we create the color variable for each sample c by flipping

$$y \text{ with probability } q^e, \text{ where } q^e = \begin{cases} 0.2 & e = e_1 \\ 0.1 & e = e_2 \\ 0.9 & e = e_0 \end{cases}.$$

The result is given in Table 1. We can observe that as n increases, the train accuracy-test accuracy gap shrinks. As p decreases, the training accuracy increases steadily. The test accuracy drops significantly in particular when p goes from 0.6 to 0.3. The reason, we think, is that the IRM is no longer able to learn a useful representation from the two training environments with completely misaligned feature representations.

E Relations between Our Bounds and Divergence-based Bounds

E.1 Review of the Divergence-based Bound for Single-Source Domain Adaptation

The seminal work by [13] considered the setting of single-source domain adaptation without representation learning, i.e., only considering \mathcal{H} but not \mathcal{F} or \mathcal{G} . It gives a bound on the risk in the target domain, based on the notion of \mathcal{H} -divergence. We review the divergence and the bound below.

By learning on the source, one cannot hope the learned hypothesis to generalize to arbitrary target. Therefore, some criterion is needed to measure how close the target is to the source. A naïve measurement is the L_1 distance. However, [13] pointed out the L_1 distance cannot be accurately estimated from finite samples of arbitrary distributions. Furthermore, it is a supremum over all measurable subsets while we are only interested in the risk of hypothesis from a class of finite complexity. They thus proposed to use the \mathcal{H} -divergence instead. The original bound is derived for the setting where the label $y \in [0, 1]$, the output of the hypothesis is in $\{0, 1\}$, and the loss is $\ell(y, y') = |y - y'|$. Here we give a variant of the divergence and the original bound for general loss, which is convenient for the later discussion on comparison to our bounds.

| p | n | Training accuracy (std dev.) | Test accuracy (std dev.) |
|-----|--------|---------------------------------|-----------------------------|
| 1 | 25000 | 0.7141 (0.0095) | 0.6489 (0.0163) |
| 1 | 50000 | 0.6978 (0.0057) | 0.6955 (0.0079) |
| 1 | 100000 | 0.6995 (0.0057) | 0.6986 (0.0099) |
| 0.9 | 25000 | 0.7193 (0.0126) | 0.6578 (0.0158) |
| 0.9 | 50000 | 0.7059 (0.0056) | 0.6951 (0.0136) |
| 0.9 | 100000 | 0.7033 (0.0053) | 0.7087 (0.0092) |
| 0.8 | 25000 | 0.7152 (0.0072) | 0.6823 (0.0121) |
| 0.8 | 50000 | 0.7107 (0.0053) | 0.6986 (0.0071) |
| 0.8 | 100000 | 0.7067 (0.0054) | 0.7025 (0.0092) |
| 0.7 | 25000 | 0.7347 (0.0122) | 0.6437 (0.0316) |
| 0.7 | 50000 | 0.7254 (0.0055) | 0.6724 (0.0124) |
| 0.7 | 100000 | 0.7198 (0.0032) | 0.6797 (0.0077) |
| 0.6 | 25000 | 0.7512 (0.0115) | 0.6126 (0.038) |
| 0.6 | 50000 | 0.7419 (0.0047) | 0.6332 (0.013) |
| 0.6 | 100000 | 0.7343 (0.0056) | 0.6388 (0.0161) |
| 0.5 | 25000 | 0.7767 (0.013) | 0.4915 (0.0583) |
| 0.5 | 50000 | 0.7551 (0.0067) | 0.5885 (0.0271) |
| 0.5 | 100000 | 0.7519 (0.0084) | 0.5981 (0.039) |
| 0.4 | 25000 | 0.7916 (0.0241) | 0.4089 (0.0991) |
| 0.4 | 50000 | 0.7828 (0.0152) | 0.4441 (0.0715) |
| 0.4 | 100000 | 0.7739 (0.0073) | 0.5053 (0.0392) |
| 0.3 | 25000 | 0.8356 (0.0065) | 0.2457 (0.0257) |
| 0.3 | 50000 | 0.8261 (0.0152) | 0.2756 (0.0497) |
| 0.3 | 100000 | 0.8277 (0.0078) | 0.2668 (0.0286) |
| 0.2 | 25000 | 0.8463 (0.0021) | 0.1879 (0.0095) |
| 0.2 | 50000 | 0.8444 (0.001) | 0.1801 (0.0067) |
| 0.2 | 100000 | 0.8425 (0.001) | 0.1853 (0.0054) |
| 0.1 | 25000 | 0.8465 (0.0017) | 0.1901 (0.0109) |
| 0.1 | 50000 | 0.8459 (0.0009) | 0.1717 (0.0127) |
| 0.1 | 100000 | 0.8455 (0.0007) | 0.1665 (0.0082) |

Table 1: Complete results of IRM under covariate shift. The covariate shift is created by manipulation of the data distribution described in the text in Section D.

Definition 12. Denote the difference between the risks of two hypotheses h, h' as

$$\nu_e(h, h') = |R^e(h) - R^e(h')|. \quad (5)$$

The generalized $\mathcal{H}\Delta\mathcal{H}$ -divergence between two distributions e, e' is

$$d_{\mathcal{H}\Delta\mathcal{H}}(e, e') = 2 \sup_{h, h' \in \mathcal{H}} |\nu_e(h, h') - \nu_{e'}(h, h')|. \quad (6)$$

The generalized divergence upper bounds the change of the hypothesis risk difference due to distribution shifts. If it is small, then for any $h, h' \in \mathcal{H}$ where h has a smaller risk than h' in e , we know that h will also have a smaller (or not too larger) risk than h' in e' . That is, if the divergence is small, then the ranking of the hypotheses w.r.t. the risk is roughly the same in both distributions. This *rank-preserving* property makes sure that a good hypothesis learned in one domain will also be good for another.

Theorem 3. Suppose the loss is non-negative. For any $h \in \mathcal{H}$,

$$R^t(h) \leq \inf_{h^* \in \mathcal{H}} \{R^t(h^*) + R^s(h^*)\} + R^s(h) + d_{\mathcal{H}\Delta\mathcal{H}}(s, t). \quad (7)$$

Proof. By definition of $d_{\mathcal{H}\Delta\mathcal{H}}(s, t)$ and non-negativity of the loss,

$$d_{\mathcal{H}\Delta\mathcal{H}}(s, t) \quad (8)$$

$$\geq \sup_{h^* \in \mathcal{H}} \{|\nu_t(h, h^*) - \nu_s(h, h^*)|\} \quad (9)$$

$$\geq \sup_{h^* \in \mathcal{H}} \{R^t(h) - R^t(h^*) - R^s(h) - R^s(h^*)\}. \quad (10)$$

Rearranging the terms completes the proof. \square

E.2 Comparing Our Single-Source Bound to the Divergence-based Bound

We can derive a bound by first applying the divergence-based bound Theorem 3 on the hypothesis class $\mathcal{H} = \{f_\phi^s \circ \phi, f_\phi^t \circ \phi\}$, and then bounding the divergence with our notions $\text{KL}_\phi^{s,t}$, $\text{KL}_\phi^{t,s}$, $\delta_\phi^{s,t}$, and $\mu_\phi^{s,t}$.

Proposition 6.

$$R^t(f_\phi^s \circ \phi) \leq 3R^s(f_\phi^s \circ \phi) + \max\{\text{KL}_\phi^{s,t}, \text{KL}_\phi^{t,s}\} + \delta_\phi^{s,t} + \mu_\phi^{s,t}.$$

Proof. Recall $\text{KL}_\phi^{t,s} = R^s(f_\phi^t \circ \phi) - R^s(f_\phi^s \circ \phi)$ and $\text{KL}_\phi^{s,t} = R^t(f_\phi^s \circ \phi) - R^t(f_\phi^t \circ \phi)$. Applying the divergence-based bound Theorem 3 on the hypothesis class $\mathcal{H} = \{f_\phi^s \circ \phi, f_\phi^t \circ \phi\}$ gives:

$$R^t(f_\phi^s \circ \phi) \leq R^s(f_\phi^s \circ \phi) + \min_{h \in \mathcal{H}} \{R^s(h) + R^t(h)\} + |\text{KL}_\phi^{t,s} - \text{KL}_\phi^{s,t}|.$$

If $\text{KL}_\phi^{t,s} \geq \text{KL}_\phi^{s,t}$, then

$$\begin{aligned} \min_{h \in \mathcal{H}} \{R^s(h) + R^t(h)\} + |\text{KL}_\phi^{t,s} - \text{KL}_\phi^{s,t}| &\leq \text{KL}_\phi^{t,s} - \text{KL}_\phi^{s,t} + R^s(f_\phi^s \circ \phi) + R^t(f_\phi^s \circ \phi) \\ &\leq \text{KL}_\phi^{t,s} + R^s(f_\phi^s \circ \phi) + R^t(f_\phi^s \circ \phi). \end{aligned}$$

If $\text{KL}_\phi^{t,s} \leq \text{KL}_\phi^{s,t}$, then

$$\begin{aligned} \min_{h \in \mathcal{H}} \{R^s(h) + R^t(h)\} + |\text{KL}_\phi^{t,s} - \text{KL}_\phi^{s,t}| &\leq -\text{KL}_\phi^{t,s} + \text{KL}_\phi^{s,t} + R^s(f_\phi^t \circ \phi) + R^t(f_\phi^t \circ \phi) \\ &\leq \text{KL}_\phi^{s,t} + R^s(f_\phi^s \circ \phi) + R^t(f_\phi^s \circ \phi). \end{aligned}$$

Then the statement follows from $R^t(f_\phi^s \circ \phi) - R^s(f_\phi^s \circ \phi) = \delta_\phi^{s,t} + \mu_\phi^{s,t}$. \square

Our bound in Theorem 1 is an equality and thus tighter than this, and the proof is simpler and more intuitive. The above proposition also shows that our bound gives a finer-grained analysis than the divergence-based bound Theorem 3.

It is also instructive to apply Theorem 3 to explain Example 1. If we apply it to $\mathcal{H} = \mathcal{F} \circ \mathcal{G}$, then we can see that the first two terms $\inf_{h^* \in \mathcal{H}} \{R^t(h^*) + R^s(h^*)\}$ and $R^s(h)$ can be small. However, $d_{\mathcal{H}\Delta\mathcal{H}}(s, t)$ will be large. Therefore, the bound can detect that the learned model may not generalize to the target domain, but it doesn't point out what leads to the problem, while our bound points out that the representation conditional label misalignment does. Furthermore, the subtle issue in Example 1 arises when one applies Theorem 3 on the representation level instead of the input level. More precisely, if we apply it on $\mathcal{H}_1 = \mathcal{F} \circ \{\phi_1\}$, we have

$$R^t(f \circ \phi_1) \leq \inf_{f^* \in \mathcal{F}} \{R^t(f^* \circ \phi_1) + R^s(f^* \circ \phi_1)\} + R^s(f \circ \phi_1) + d_{\mathcal{H}_1 \Delta \mathcal{H}_1}(s, t). \quad (11)$$

Similarly, if we apply it on $\mathcal{H}_2 = \mathcal{F} \circ \{\phi_2\}$, we have

$$R^t(f \circ \phi_2) \leq \inf_{f^* \in \mathcal{F}} \{R^t(f^* \circ \phi_2) + R^s(f^* \circ \phi_2)\} + R^s(f \circ \phi_2) + d_{\mathcal{H}_2 \Delta \mathcal{H}_2}(s, t). \quad (12)$$

The last two terms can be made small, but the generalization gap gets hidden in the first term. In particular, both $d_{\mathcal{H}_1 \Delta \mathcal{H}_1}(s, t)$ and $d_{\mathcal{H}_2 \Delta \mathcal{H}_2}(s, t)$ are 0, but $d_{\mathcal{H}\Delta\mathcal{H}}(s, t)$ can be large. Note that though $\mathcal{H} = \mathcal{H}_1 \cup \mathcal{H}_2$, $d_{\mathcal{H}\Delta\mathcal{H}}(s, t)$ is much larger than the maximum of $d_{\mathcal{H}_1 \Delta \mathcal{H}_1}(s, t)$ and $d_{\mathcal{H}_2 \Delta \mathcal{H}_2}(s, t)$. The difference between $d_{\mathcal{H}\Delta\mathcal{H}}(s, t)$ and $\max\{d_{\mathcal{H}_1 \Delta \mathcal{H}_1}(s, t), d_{\mathcal{H}_2 \Delta \mathcal{H}_2}(s, t)\}$ gets hidden in the first term, and is the root for the subtle issue in Example 1. In summary, using the bound on the input level is the correct way to apply it, which can detect there is an issue for generalization but still doesn't point out where the issue comes from.

E.3 Generalizing the Divergence-based Bound to Multi-Source Domain Adaptation

Here we show one can generalize the divergence-based bound for the case with a single source s and target t to the case with multiple sources \mathcal{E}_{tr} and a target e_0 .

Based on the divergence, we introduce the key notion for the analysis:

Definition 13. *The \mathcal{H} -misalignment from e_0 to \mathcal{E}_{tr} is*

$$d_{\mathcal{H}}(e_0; \mathcal{E}_{\text{tr}}) = \inf_{e \in \mathcal{E}_{\text{tr}}} \left\{ \frac{1}{2} d_{\mathcal{H}\Delta\mathcal{H}}(e_0, e) \right\} = \inf_{e \in \mathcal{E}_{\text{tr}}} \sup_{h, h' \in \mathcal{H}} |\nu_{e_0}(h, h') - \nu_e(h, h')|. \quad (13)$$

The notion measures how aligned e_0 is to \mathcal{E}_{tr} w.r.t. risk ranking. Intuitively, as long as there exists one $e \in \mathcal{E}_{\text{tr}}$ whose ranking of the hypotheses by their risks is similar to that of e_0 , then e_0 is aligned to \mathcal{E}_{tr} . To emphasize the difference from typical distribution distances, we use the term misalignment instead.

Then we can generalize Theorem 3 as follows.

Theorem 4. *Suppose the loss is non-negative. For any e_0 and any $h \in \mathcal{H}$,*

$$R^{e_0}(h) \leq \inf_{h^* \in \mathcal{H}} \left\{ R^{e_0}(h^*) + \sup_{e \in \mathcal{E}_{\text{tr}}} R^e(h^*) \right\} + \sup_{e \in \mathcal{E}_{\text{tr}}} R^e(h) + d_{\mathcal{H}}(e_0; \mathcal{E}_{\text{tr}}). \quad (14)$$

Proof. By definition of $d_{\mathcal{H}}(e_0; \mathcal{E}_{\text{tr}})$ and non-negativity of the loss,

$$d_{\mathcal{H}}(e_0; \mathcal{E}_{\text{tr}}) \quad (15)$$

$$\geq \inf_{e \in \mathcal{E}_{\text{tr}}} \sup_{h^* \in \mathcal{H}} \{|\nu_{e_0}(h, h^*) - \nu_e(h, h^*)|\} \quad (16)$$

$$\geq \inf_{e \in \mathcal{E}_{\text{tr}}} \sup_{h^* \in \mathcal{H}} \{R^{e_0}(h) - R^{e_0}(h^*) - R^e(h) - R^e(h^*)\}. \quad (17)$$

Applying the maxmin inequality and then rearranging the terms completes the proof. \square

Similar to the single-source case, the bound in Theorem 4 uses $\inf_{h^* \in \mathcal{H}} \{R^{e_0}(h^*) + \sup_{e \in \mathcal{E}_{\text{tr}}} R^e(h^*)\}$ and $d_{\mathcal{H}}(e_0; \mathcal{E}_{\text{tr}})$. While our bound in Theorem 2 uses our notions of representation conditional label divergence, representation covariate shift, and prediction adaptation gap. The terms in Theorem 4 can also be bounded using our notions using a similar argument as in Proposition 6. Therefore, compared to the divergence-based bound, our bound provides a finer-grained analysis in the setting of representation learning.